NOVATEUR PUBLICATIONS
JournalNX- A Multidisciplinary Peer Reviewed Journal
ISSN No: 2581 - 4230
VOLUME 8, ISSUE 7, July -2022

REMOTE SENSING UTILIZATION FOR THE MODELLING OF LAND SURFACE TEMPERATURE FOR SUSTAINABLE CITY DEVELOPMENT

Israa Fadhil Ibraheem
Surveying Techniques Engineering Department / Technical Engineering College
Baghdad Middle Technical University –Baghdad/Iraq, Baghdad, Iraq
asraafadhil2000@gmail.com

Mufid Al-hadithi
Surveying Techniques Engineering Department / Technical Engineering College
Baghdad Middle Technical University –Baghdad/Iraq, Baghdad, Iraq
mufidalhadithi@yahoo.com

ABSTRACT
Land Surface Temperature (LST) is a critical input for climatological, hydrological, agricultural, and change detection models. In the current study, Baghdad LST was evaluated using remotely sensed thermal infrared data. This study examines the extraction of both land surface emissivity (LSE) and LST from images taken on October 2001, October 2013 and October 2021 across the study area, as well as the link between vegetation abundance. To calculate LST over the study region, the Plank equation was utilized and the variety of LSE was explored and retrieved using the NDVI threshold approach. The findings show that in 2001, 2013 and 2021, respectively, the Land Surface Temperature (LST) ranges from 52 to 11, 53 to 23 and 59 to 29 degrees Celsius. Barren area had the lowest LSE value, while the lush vegetation had the highest LSE value, which was equivalent to 0.99. Ground observation points and Google Earth imagery were used for accuracy assessment of LULC maps. Barren land and building areas are associated with the highest temperatures that range from 52, 53, and 59degrees Celsius, while forests and water bodies have lower temperatures that range from 11, 23, and 29 degrees Celsius respectively, in 2001, 2013 and 2021. Also, the research reveals that low temperatures have a negative correlation with NDVI and NDWI, conversely high temperatures have a positive correlation with BUI.

Keywords: LST;NDVI; LSE; NDWI; NDBI , BUI.

I. INTRODUCTION

Growing industrialization and urbanization are key factors contributing to climate change. The most pressing issue currently facing urban regions is the rise in surface temperatures brought on by the expansion of non-transpiring, impermeable, hard non-evaporating land surfaces on the behalf of vegetated areas. Remote sensing key application in the study of urban climate is the analysis of the relationship among urban surface characteristics, spatial structure and urban thermal patterns using land surface temperature (LST), which is aided by sensors data from remote sensing's thermal infrared bands [1].

In order to alter land use, like urban land, vegetation land and other human uses, many natural land coverings have been removed. The term "LUCC" refers to the conversion of lands from one land use to other type. as a result of the composite relationship between the environment and anthropogenic influences [2]. In addition to having a substantial impact on ecosystem change, LST change, the

biodiversity cycle, and biodiversity, LUCC considered as a significant contributor to the change in global environmental [3].

LST can be calculated from radiance readings taken by weather stations. Since it is a point-based measurement, a large-scale monitoring doesn't permit in this method typically [4,5]. Remotely sensed TIR data enable large-scale, even global, temporal and spatial LST investigation [6]. According to atmospheric factors, sensor characteristics like angle of view and spectral range, and surface characteristics like emissivity and shape, accurate LST retrieval from TIR data is dependent [7–8]. Since emissivity and atmospheric influences are two essential variables for determining LST from thermal data, numerous studies have suggested various methods for LST retrieval taking these variables into account [9–10]. The number of TIR bands utilized is taken into account when naming these algorithms. For instance, one TIR band is used by single-channel or mono-window algorithms. However, many TIR bands are used in split window or multi-channel systems.

Land use change monitoring could be viewed as an alternative kind of adequate administration for the accomplishment of sustainable development [11,12]. According to studies, urban microclimates changed as a result of increased urban expansion and a corresponding decline in vegetation [13]. The association between vegetation abundance and land surface temperature was established by another study. Numerous vegetation indicators, including the fractional vegetation cover and normalized vegetation index, show that there is an abundance of vegetation (NDVI). As a result of the changes in soil moisture, the abundance of vegetation, land surface emissivity, and albedo an inverse relationship between NDVI and land surface temperature in addition to agricultural areas cooling effect have been found [14,15]. This has led to a decrease in the dense vegetation variable temperatures [16]. Political and socioeconomic trends have a significant impact on urban expansion [8,16,18]. As a result, the example of the rapidly expanding metropolitan region of Baghdad Governorate in Iraq was chosen in order to calculate LST from Landsat-7 and 8 satellite datasets for the study region (Baghdad Governorate, Iraq) throughout the time period (2001-2013-2021) and to link LST with NDVI, NDWI and BUI in order to construct reliable linear models.

II. STUDY AREA

Some districts and counties in the Baghdad Governorate are included in the study area (Fig.1). Iraq's capital Baghdad is a significant hub for scientific research, education, and industry, and it has a high level of urbanization and it's estimated population in 2021 is about 4 million. In order to comprehend, manage, and plan the future development of the city, it is important to explored the connection between LST and urban expansion in the area of interest, which is situated between 33°10′ and 33°30N and 44°14′ and 44°33′E.

From the USGS Earth Resource Observation Systems Data Centre, a cloudless Landsat 8 OLI (Operational Land Imager) and TIRS (Thermal Infrared Sensor) image, collected in October 2013 and 2021 (PATH/ROW: 168/37) was downloaded. Before delivery, the geometrical and radiometric deviation were rectified to a 1 T quality level. Following that, FLAASH atmospheric correction was used to pre-process OLI's multispectral data. The pixel size of the resampled thermal infrared data from TIRS was 30 m 30 m.

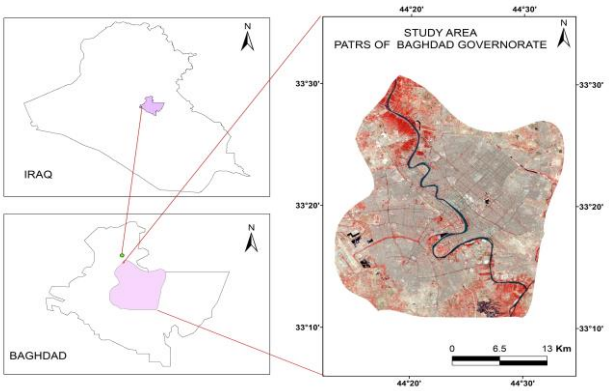

Fig. 1. Location of Study Area

A. Source of Data

- Landsat Imagery Data

The first Landsat ETM-7 image was dated on October 5, 2001. The second and third Landsat OLI TIRS-8 images were dated on October 14, 2013 and October 4, 2021. In this research, all bands were utilized, particularly the prominent thermal bands for locating LST (Table I).

- Measurements of Ground Soil Temperature

The closest correlation between soil temperature and LST is seen at a depth of roughly 5 cm, according to in situ soil temperature studies . For the purpose of evaluating the satellite-derived LST, data of the soil temperature from the 20 soil temperature locations are utilized as a proxy for the surface temperature.

TABLE I. DETAILS OF LANDSAT SATELITE IMAGES

Bands (µm.)	Landsat 7 (ETM+)		Bands (µm)	Landsat 8 OLI and TIRS	
	Resolution(m)	wavelengths(µm)		Resolution(m)	wavelengths(µm)
			Band 1- Coastal/Aerosol	30m	0.435 - 0.451
Band 1– Blue	30m	0.45 - 0.52	Band 2 /Blue	30 m	0.452 - 0.512
Band 2 – Green	30m	0.52 - 0.60	Band 3/Green	30 m	0.533 - 0.590
Band 3– Red	30m	0.63 - 0.69	Band 4/ Red	30 m	0.636 - 0.673
Band 4– (NIR)	30m	0.77- 0.90	Band 5/ NIR	30 m	0.851- 0.879
Band 5- (SWIR)1	30m	1.55 - 1.75	Band 6/SWIR-1	30 m	1.566 - 1.651
Band 6– TIR	60m	10.40 - 12.50	Band 10/TIR-1	100 m	10.60 - 11.19
Band 7- (SWIR)2	30m	2.09 - 2.35	Band 11/ TIR-2	100 m	11.50 - 12.51
Band 8- Pan	15m	0.52 - 0.90	Band 7/ SWIR-2	30 m	2.107 - 2.294
			Band 8/ Pan	15 m	0.503 - 0.676
			Band 9/ Cirrus	30 m	1.363 - 1.384

B. Methodology

Several methods were utilized in this research for the Landsat images analyzation: (1) Images calibration for radiometric and geometric errors; (2) derivation of top atmospheric temperature and brightness; 3 derivations of NDVI and NDBI, BUI after the atmospheric correction for all bands; (4) retrieval of the LST for each image; (4) After conversion to vector all files will be insert into ArcGIS for calculations and manipulation through attribute tables (Fig. 2).

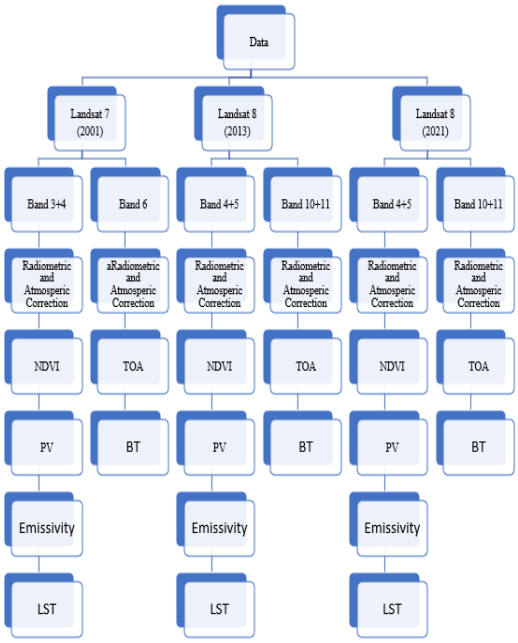

Fig. 2. Methodology Flowchart

- Image Classification and Accuracy Analysis

LULC classification is crucial for studying the regional effects of human actions because it allows for the detection of changes in land use along time of the research. For 2001, 2013, and 2021, LULC changes were mapped using Landsat imagery. The four LULC types chosen are water, vegetation-covered land, built-up regions, and barren area. In order to create training sites based on auxiliary data and reference data from multiple sources, the images were examined in accordance with their spectral and spatial profiles. For each land cover class, this study allocated 50 training samples made up of 50 pixels. For each land cover category, 20 training samples of 50 pixels are required [19].

After digitalization of training sites, the various land cover groups statistical characteristics were created. The maximum likelihood technique was then used to classify Landsat images after extracting supervised signatures. Using stratified random sample techniques, the accuracy of the three categorized maps was evaluated. Twenty samples from each LULC class were selected. In addition to LULC maps that were field validated, a field survey served as reference data.

- NDVI and NDBI, BUI Computation

In comparison to another indices, NDVI is less influenced by atmospheric factors changes, so LST studies frequently employ this metric to monitor the status of the vegetation [20]. In this work, Band 4,5 and 7 were corrected from atmospheric impact and linear regression correlation method was employed to show the association between LST and vegetation area. NDVI is calculated as follows:

NDVI=(NIRμm-REDμm)/(NIRμm+REDμm) …….(1)

A common index for assessing built-up statuses is the NDBI and BUI [10,21]. NDBI values can range from the near infrared region to the middle infrared based on the spectral signature. It is helpful for various aspects of nearby constructions in addition to mapping human settlements [22].

The Normalized Difference Water Index (NDWI) [23] suggests that vegetation has a water condition and contains water. NDWI and BUI values could be range from (-1 - +1). Positive numbers represent water features and densely populated areas, whereas negative values show various types of land cover. This index is computed using the following formula:

NDWI=(NIRμm-SWIRμm)/(NIIRμm+SWIRμm) …….(2)
NDBI=(SWIRμm-NIRμm)/(SWIRμm+NIRμm) …….(3)
BUI=NDBI-NDVI …….4

- LST Computation

Landsat satellite thermal infrared data with spatial resolutions of 60 m and 100 m were used to produce Land Surface Temperature (LST) maps. To detect radiation from the earth's surface, thermal infrared band was used [24]. Two steps are needed for derived LST: First, using the following formula, DN of Landsat images for the conversion to Top-of-Atmosphere (TOA) radiance:

L(λ)=(ML×Band10+AL-Oi)/sin〖(elevation)〗 …….5 L(λ)=(ML×Band111+AL-Oi)/sin〖(elevation)〗 …….6

Where:
L(λ): spectral radiance for TOA
ML: Radiance multiplicative band (from MTL txt.)
AL: Radiance add Band 10, Band 11(from MTL txt.)
Oi: correction value (for Landsat 8 Band 10 its = 0.29)
Radiance Mult. Band10, Band 11 = 0.000342
Radiance Add Band10, Band 11 = 0.10000
The second step includes transformation of Spectral Radiance into Temperature in Kelvin:

$$\text{Kelvin (k) to Celsius degree Co BT} = \frac{K2}{\ln\left(\frac{K1}{L(\lambda)}+1\right)} - 273.15 \quad \ldots\ldots 6$$

Where:

- BT: Top of Atmosphere brightness temperature Co
- L(λ): spectral radiance of TOA
- K1: Calibration Constant for Band 10 = 774.8853
- K1: Calibration Constant Band 11= 480.8883
- K2: Calibration Constant for Band10 = 1321.0789
- K2: Calibration Constant for Band 11= 1201.1442

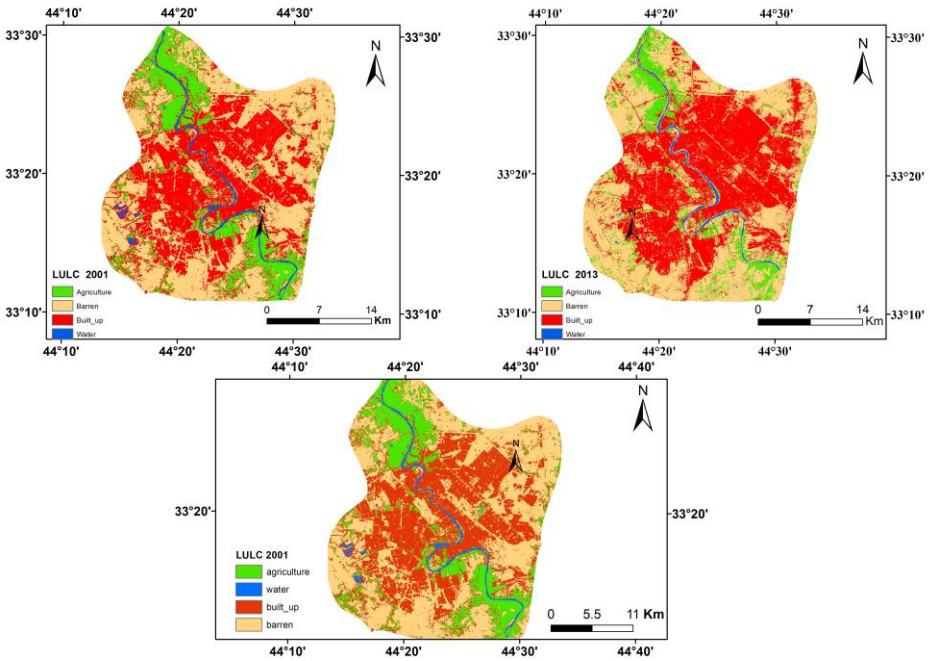

Fig. 3. Classification Map of LU/LC

III. RESULTS AND DISCUSSION

The outcomes of the research include study area maps of land use and land cover, the distribution of land surface temperatures, and the NDVI, BUI and NDWI.

A. Maps of Land Use/Land Cover

In order to accurately produce the LULC map in 2001, 2013, and 2021, maximum likelihood for supervised classification was employed. The precise area of LULC of the study area is recorded in TABLE II and Fig. 3, and it is roughly (820.12) Km^2 in size.

TABLE II. DETAILS OF LANDSAT SATELITE IMAGES

Type of use	2001		2013		2021	
	Km^2	%	Km^2	%	Km^2	%
Vegetation	140.26	17%	84.35	10%	63.89	8%
Barren	355.38	43%	370.96	45%	122.72	15%
Building	308.92	38%	354.59	43%	623.93	76%
Water	15.57	2%	10.22	1%	9.58	1%
	820.12	100%	820.12	100%		100%

Alteration in LULC, particularly in urbanized regions where they have expanded considerably, were responsible for LST changes. TABLE II demonstrates that between 2001 and 2013, the building categories that include (residential, administrative buildings and commercial) increased marginally by 13 percent, from (308.92Km^2) to (354.59Km^2), while a notable increase was observed between 2013 and 2021, growing by 43 percent from 354.59Km^2 to 623.93Km^2.

There are numerous reasons influencing the growth of urbanized areas; significant changes occurred in the outskirt of urban areas. Since 2003, the research area witnesses significant changes as a result of political and socioeconomic variables (TABLE II). These areas were extensively developed by the government and/or private corporations for a variety of retail, industrial, and residential uses, which has also contributed to the decrease in the amount of deserted land surrounding the city. These structures were built using impermeable materials like concrete and steel frames. Conversely the bare area decreased from 355.38 Km^2 to 370.69Km^2 through the years 2001 - 2013, and decreased by 66.8 percent from 370.69Km^2 to 122.72 Km^2 through 2013 - 2021, whereas the area covered by water and vegetation decreased by 34.4 percent and 40 percent from 15.57Km^2 to 10.22Km^2 and from 140.62Km^2 to 84.35Km^2, respectively, and by 3.48 percent and 0.05 percent, respectively, from 2001 to 2013. The study's findings also show that green areas and water bodies decreased from 84.35$Km^2$and 10.22Km^2, respectively in 2013 to 63.89Km^2 and 9.58Km^2 in 2021.

B. Land Surface Temperature extraction

The study area absolute LST map of is the end result of the investigation. Fig. 4, 5,6 are an illustration of the computed LST map. In 2001, 2013, and 2021, LST indicated value varying from (11-52) degrees Celsius, (23-53) degrees Celsius, and (29-59) degrees Celsius respectively. The increase in maximum LST for the entire region was 7 degrees Celsius from 52 degrees Celsius, 53 degrees Celsius, and 59 degrees Celsius in 2001, 2013, and 2021, respectively. At the same time, the increased in lowest temperature was 18 degrees Celsius from 11 degrees Celsius, 23 degrees Celsius, and 29 degrees Celsius. The 2001 images were taken on October 18, 2001, the 2013 images on October 13, 2013, and the 2021 images on October 4, 2021. Climate change may be the cause for these shifts.

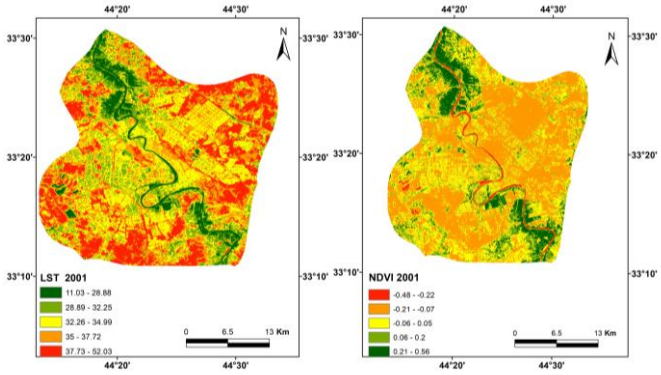

Fig. 4. LST & NDVI Maps in 2001

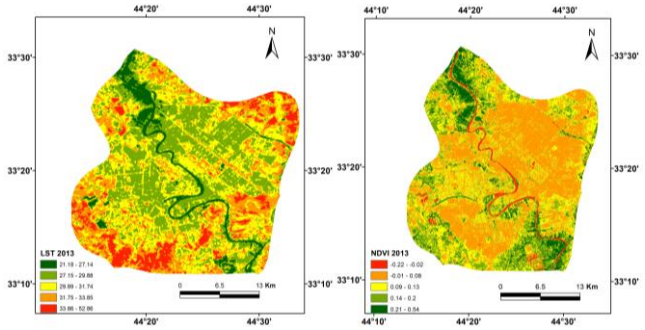

Fig. 5. LST & NDVI Maps in 2013

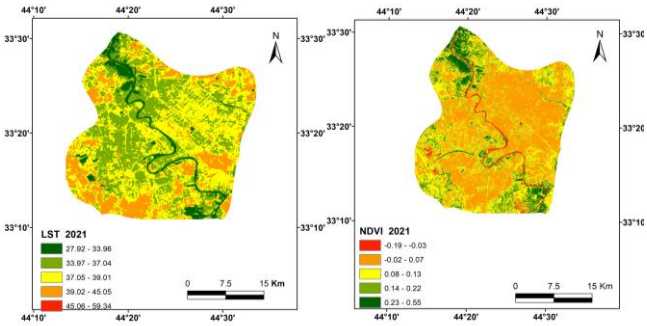

Fig. 6. LST & NDVI Maps in 2021

C. Different Land Covers and Land Surface Temperature Relation

To comprehend the connection between LST and land cover, it is crucial to investigate each LULC type's thermal signature [13]. In order to compare LULC and LST, for each LULC classes in the area of research, sampling points were chosen and the LST values were then compared. The average of all consistent pixels within a specific LULC category was used to determine the mean temperature for each land use/cover group. The data showed that rock outcrops had the highest LST, whilst aquatic bodies had the lowest. The coldest anchor pixels were found near vegetation and water, while the hottest were found near rock, populated regions, or barren soils. This study found that temperatures were greater outside and in the undeveloped regions of the city than they were inside. As a result, the LST findings of this study might be at odds with those of earlier studies [2,25], which indicate that urban areas have greater LST values than suburban and rural locations. As a result of the sun's heat being immediately absorbed by the surrounding areas, which causes it to heat up more quickly compared to other categories of land cover, Baghdad City demonstrated a lower LST in urban areas

during the study period than in suburbs (Figs.4-6). Roads, buildings, concrete, pavements, and other elements that comprise urban surfaces, on the other hand, have a tendency to gradually release the heat that was absorbed. In another words, compared to other land cover classifications, like barren ground on the outskirts, which doesn't keep heat for as long, building land tends to retain heat longer. This study finding demonstrate that arid lands and the surrounding areas are hotter than urban areas; this result may be related to the date of the image acquisition. LST with lower values were recorded in building regions in comparison with barren areas because urban surfaces absorb temperature more slowly and features in building areas cool down and warm up more slowly than other categories of land cover, like barren land. Despite this, because each form of land has different energy radiation and absorption characteristics, the shifting of the LST is also a result of changes in the land. Building lands have a higher absorption and lower albedo than barren lands because of the higher temperatures in the surrounding areas and arid lands than in metropolitan areas. These results are consistent with those of [2], who found that places with bare soil and building sectors have greater LST values during the daytime in comparison with other categories including water bodies, agricultural, and vegetation. Building and arid environments, on the other hand, have lower LST values at night, while it is noted that LST values are higher in water and agricultural bodies.

Each LULC class's LST is consequently determined by its unique feature. It was demonstrated that the most effective way to explore the link between land cover types and thermal signatures and different types of land cover [3]. Fifty randomly points have been chosen to investigate the relationship among the NDVI, BUI, and NDWI obtained from Landsat ETM-7 2001 and Landsat OLI TIRS-8 2013, 2021, respectively and LST using sample point method. Figs. 7–15 illustrate the degree of linkage and connections among the LST, NDVI, BUI, and NDWI. These associations were analyze using Pearson's correlation coefficient analysis. It is evident from the result that regions with higher temperatures as well as greater BUI have lower NDVI and NDWI values. However, BUI derived building fractions and the surface temperature (LST) showed a positive link, with correlation coefficients of R2 = 0.8615, 0.855, and 0.9493 demonstrated in all images. The results of the linear correlation revealed a positive linkage between the LST and BUI derived bare land fractions, as indicated by correlation coefficients of R2 = 0.815, 0.803, and 0.85.

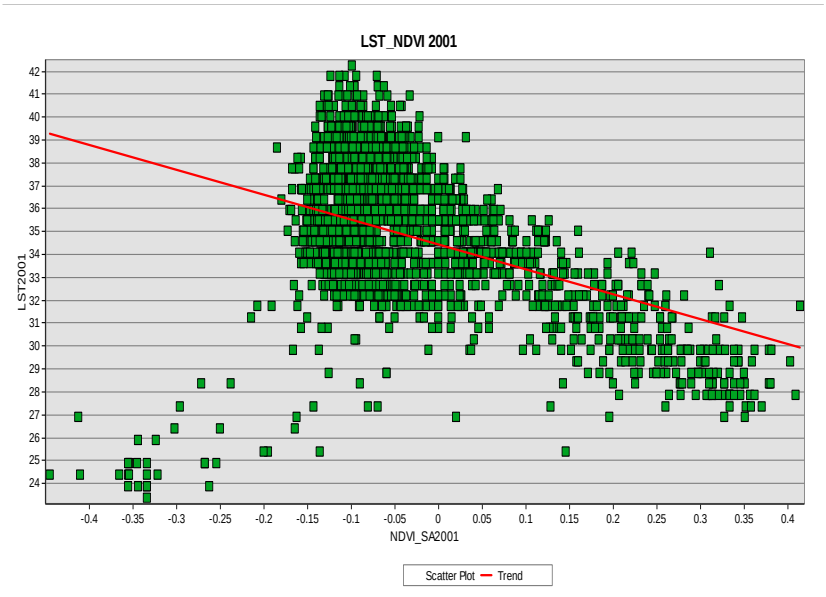

Fig. 7. LST & NDVI Correlation in 2001

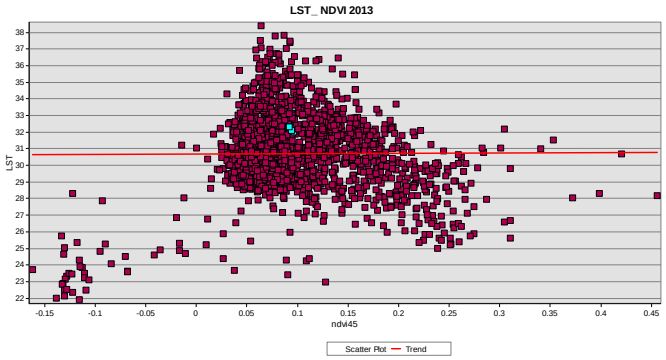

Fig. 8. LST & NDVI Correlation in 2013

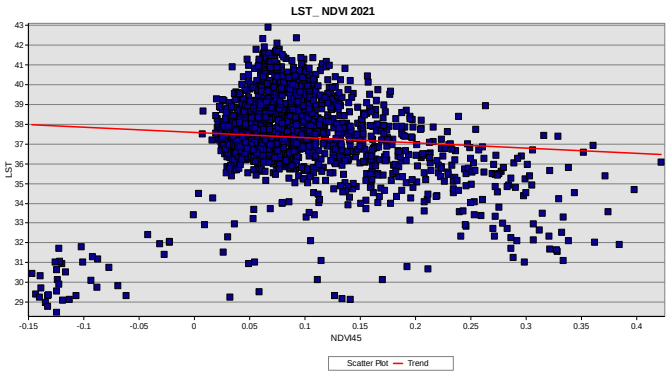

Fig. 9. LST & NDVI Correlation in 2021

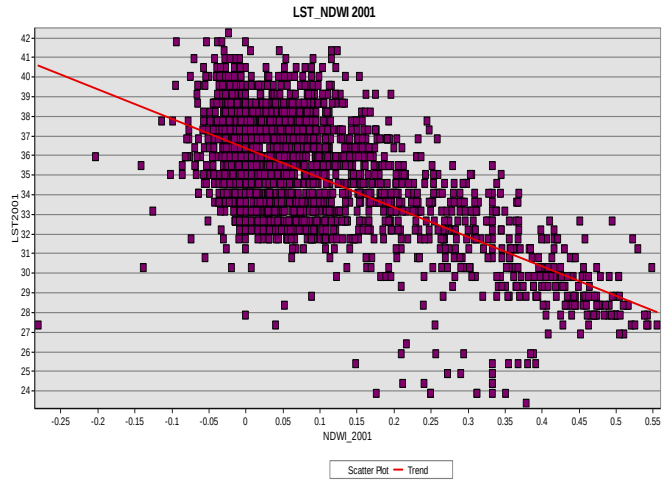

Fig. 10. LST & NDWI Correlation in 2001

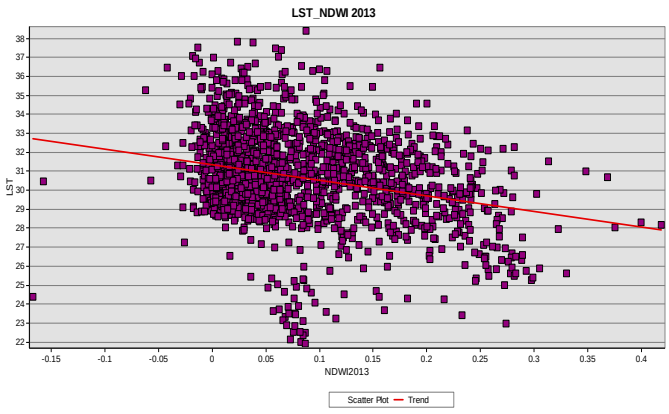

Fig. 11. LST & NDWI Correlation in 2013

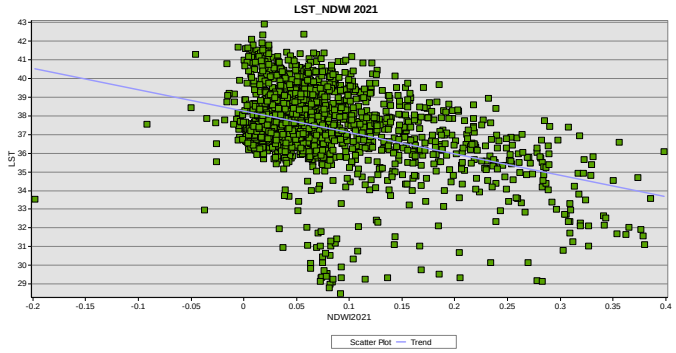

Fig. 12. LST & NDWI Correlation in 2021

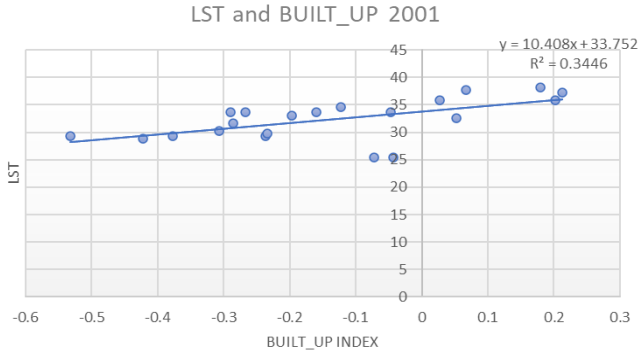

Fig. 13. LST & BUILT_UP INDEX Correlation in 2001

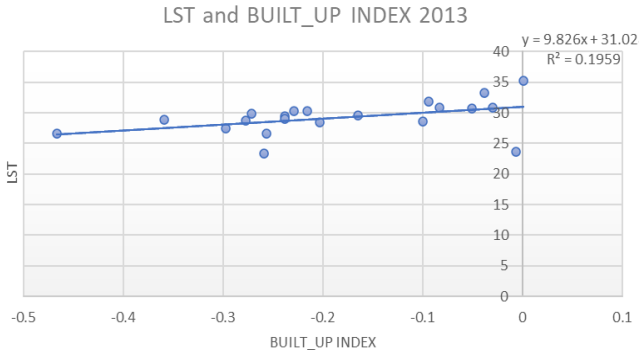

Fig. 14. LST & BUILT_UP INDEX Correlation in 2013

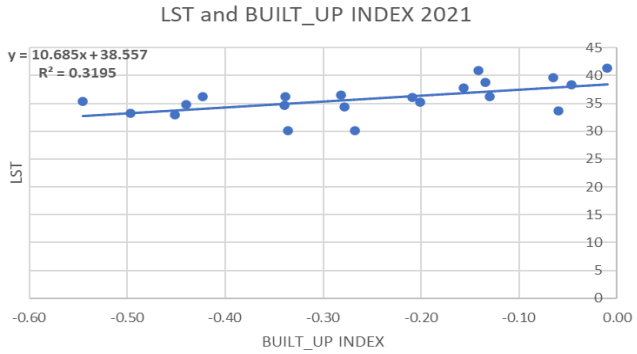

Fig. 15. LST & BUILT_UP INDEX Correlation in 2021

IV. CONCLUSIONS

This study used multi-temporal remote sensing data and relies on it to track alterations in land use /land cover along with their affect Baghdad Governorate LST. This study aims were successfully attained by the applied strategies used in this investigation. The study made an effort to pinpoint

changes in classes of land use and how they affected LST. Urban areas, dry land, vegetated areas, and water bodies were used to categorize the study area. Regarding to land cover classification results, political and socio-economic factors caused the water bodies and building areas to grow by 0.1 percent and 12.02 percent, respectively, during the study period, while vegetation and the barren land shrank by 1.46 percent and 1.63 percent, respectively. It is clear that LST and LULC are closely related. The study demonstrated that the Various categories of land cover have different LST values; for instance, metropolitan regions and wastelands had higher radiant temperatures. Earlier research which found greater LST amount in urban regions than in rural and suburban sectors may be in conflict with rising temperatures outside of the city rather than within its boundaries and in areas without built-up areas. This is a result of the high temperatures of cities especially in summer. Urban expansion has a negative effect on LST due to changes in the natural characteristics of the land cover, consists of placing the vegetation in building areas, due to the city's semi-arid environment. Additionally, the study discovered a negative correlation between the land surface temperature and the amount of vegetation (NDVI) and water bodies (NDWI). impacted by the LULC and highly sensitive to soil moisture and vegetation; in particular, it was found that the amount of vegetation is the major variable on which this relationship is based. Although research indicated a positive association among LST, and BUI less vegetated LULC areas exhibit greater LST, and vice versa.

REFERENCES

1. Y. Kant, B. D. Bharath, , J.Mallick, , C.Atzberger, & N.Kerle, Satellite-based analysis of the role of land use/land cover and vegetation density on surface temperature regime of Delhi, India. Journal of the Indian Society of Remote Sensing, **2009,** pp.201-214. [CrossRef]
2. S. N. A.Buyadi, W. M. N. W.Mohd, & A.Misni, Impact of land use changes on the surface temperature distribution of area surrounding the National Botanic Garden, Shah Alam. Procedia-Social and Behavioral Sciences, 2013, pp. 516-525. [CrossRef](6)
3. Q. Weng, A remote sensing and GIS evaluation of urban expansion and its impact on surface temperature in the Zhujiang Delta, China. International journal of remote sensing, 2010, pp.1999-2014. [CrossRef]
4. F. Becker, & Z. L. Li, Surface temperature and emissivity at various scales: Definition, measurement and related problems. Remote sensing reviews, 1995, pp.225-253. [CrossRef]
5. R. C.Hale, K. P.Gallo, D.Tarpley, & Y. Yu, Characterization of variability at in situ locations for calibration/validation of satellite-derived land surface temperature data. Remote Sensing Letters, 2011,pp. 41-50. [CrossRef]
6. C. Gao, X. Jiang, , Z. L.Li, & F. Nerry, Comparison of the Thermal Sensors of SEVIRI and MODIS for LST Mapping. In Thermal Infrared Remote Sensing,2013, pp. 233-252.
7. P. Dash, F. M. Göttsche, F. S. Olesen, & H. Fischer, Retrieval of land surface temperature and emissivity from satellite data: physics, theoretical limitations and current methods. Journal of the Indian Society of Remote Sensing, 2001, pp.23-30 [CrossRef]
8. S. Chen, S. Zeng, & C. Xie, Remote sensing and GIS for urban growth analysis in China. Photogrammetric Engineering and Remote Sensing, 2000 ,pp.593-598.
9. D. Ghent, K. Veal, T. Trent, E. Dodd, H. Sembhi, & J. Remedios, A new approach to defining uncertainties for MODIS land surface temperature. Remote Sensing, 2019,pp. 1021.

10. X. Yu, X. Guo, & Z.Wu, Land surface temperature retrieval from Landsat 8 TIRS—Comparison between radiative transfer equation-based method, split window algorithm and single channel method. Remote sensing, 2014 pp. 9829–9852. [CrossRef]
11. M. Zurina, & S. Hukil, Appraising good governance in Malaysia based on sustainable development values. Journal of ASIAN Behavioural Studies: Sustainability Science and Management, 2012, pp. 247-253.
12. F. Alqaisi, The effects of stakeholder's engagement and communication management on projects success. In MATEC Web of Conferences 2018 ,Vol. 162, p. 02037.
13. H. Geist, W. McConnell, E. F. Lambin, E. Moran, D. Alves, & T. Rudel, Causes and trajectories of land-use/cover change. In Land-use and land-cover change 2006, pp. 41-70.
14. J. Jiang, & G. Tian, Analysis of the impact of land use/land cover change on land surface temperature with remote sensing. Procedia environmental sciences, 2010, pp.571-575. [CrossRef]
15. T. N. Carlson, & S. T. Arthur, The impact of land use—land cover changes due to urbanization on surface microclimate and hydrology: a satellite perspective. Global and planetary change, 2000, pp. 49-65. [CrossRef]
16. J. Huang, R. Wang, F. Li, W.Yang, , C. Zhou, J. Jin, & Y. Shi, Simulation of thermal effects due to different amounts of urban vegetation within the built-up area of Beijing, China. International Journal of Sustainable Development & World Ecology, 2009, pp.67-76. [CrossRef]
17. F.Ibraheem, , M. A. & Al-Jaafari, Evaluation of photovoltaic potential application in urban environments using GIS-based method: the particular case of Baghdad/Iraq. In IOP Conference Series: Materials Science and Engineering ,2020 ,Vol. 1105, No. 1, p. 012083).
18. N. B. Grimm, S. H. Faeth, N. E. Golubiewski, C. L. Redman, J. Wu, X. Bai, & J. M. Briggs, Global change and the ecology of cities. science, 2008, pp.756-760. [CrossRef]
19. T. M.Lillesand, , R. W. Kiefer, and J. W. Chipman. "Digital image interpretation and analysis." Remote sensing and image interpretation , 2008,pp. 545-81.
20. M. K.Raynolds, , J. C. Comiso, , D. A. Walker, , & D. Verbyla, Relationship between satellite-derived land surface temperatures, arctic vegetation types, and NDVI. Remote Sensing of Environment, 2008, pp.1884-1894.
21. Grover, & R. B. Singh, Monitoring Spatial patterns of Land Surface Temperature and urban heat island for sustainable megacity: A case study of Mumbai, India, using Landsat TM data. Environment and Urbanization ASIA, 2016, pp.38-54.
22. S. Youneszadeh, N. Amiri, & P. Pilesjo, The effect of land use change on land surface temperature in the Netherlands. The International Archives of Photogrammetry, Remote Sensing and Spatial Information Sciences, 2015, pp.745-748
23. Chunyang, P. Shi, , D. Xie, & Y.Zhao, Improving the normalized difference built-up index to map urban built-up areas using a semiautomatic segmentation approach. Remote Sensing Letters, 2010, pp.213-221.
24. Ahmed, M. D. Kamruzzaman, X. Zhu, M. S. Rahman, & K. Choi, Simulating land cover changes and their impacts on land surface temperature in Dhaka, Bangladesh. Remote sensing, 2013, pp.5969-5998.
25. V. Rodriguez-Galiano, E. Pardo-Igúzquiza, M.Sanchez-Castillo, M. Chica-Olmo, & M. Chica-Rivas, Downscaling Landsat 7 ETM+ thermal imagery using land surface temperature and NDVI images. International Journal of Applied Earth Observation and Geoinformation, 2012,pp. 515-527.